JOURNAL OF PHYSICAL ORGANIC CHEMISTRY
J. Phys. Org. Chem. 2004; **17**: 934–944
Published online 13 August 2004 in Wiley InterScience (www.interscience.wiley.com). DOI: 10.1002/poc.817

Review Commentary

Novel sugar-based gemini surfactants: aggregation properties in aqueous solution†

Markus Johnsson[1]* and Jan B. F. N. Engberts[2]

[1]Physical Chemistry 1, Chemical Center, Lund University, P.O. Box 124, SE-22100 Lund, Sweden
[2]Stratingh Institute, Physical Organic Chemistry Unit, University of Groningen, Nijenborgh 4, 9747 AG Groningen, The Netherlands

Received 8 December 2003; revised 28 January 2004; accepted 31 January 2004

ABSTRACT: Gemini or dimeric surfactants can in principle be viewed as two conventional surfactants connected via a spacer at the level of the polar headgroups. A novel class of sugar-based gemini surfactants with rich and intriguing aggregation behavior in aqueous solution is the focus of this mini-review. The headgroup of the geminis consists of reduced sugars (glucose or mannose) connected to tertiary amines or amides. The alkyl tails have been varied in terms of tail length and degree of unsaturation. The spacers used are aliphatic [—$(CH_2)_n$—] spacers of varying length or short ethylene oxide (EO) spacers [—$(CH_2)_2$—$(EO)_2$—]. By manipulating the molecular architecture and the solution conditions, a variety of supramolecular aggregates, such as vesicles and micelles, are formed from these sugar-based surfactants. In particular, the sugar-based gemini surfactants containing tertiary amines in the headgroup respond to the solution pH by forming vesicles in the monoprotonated state and micellar structures in the diprotonated (full protonation) state. The overall aggregation behavior is described well by conventional theories on surfactant aggregation, however, a surprising vesicle surface charge reversal as a function of pH will be described and discussed. Copyright © 2004 John Wiley & Sons, Ltd.

KEYWORDS: pH-dependent aggregation behavior; vesicle-to-micelle transition; dimeric surfactants; cylindrical micelles; vesicles; vesicle zeta-potential; colloidal stability; aggregate morphology

INTRODUCTION

The term gemini surfactant was coined by Menger and Littau[1] in 1991 describing a novel type of surfactant consisting of two identical conventional surfactants connected via a spacer at the level of the headgroups (Plate 1). Several other names have been suggested for this class of surfactant, including dimeric surfactants[2] and even siamese surfactants[3] alluding to the nature of their connections. The semantic issues aside, these surfactants have opened a new field of research within surface and colloid chemistry because of their unique properties when dispersed in water. Combined with an often trivial synthesis, a large-scale production of the geminis seems likely in the near future. In this respect it must be emphasized that more intricate structural variations on the 'gemini-theme' require the input of physical-organic and synthetic chemists, and there is clearly a huge potential for tailor-making of geminis exhibiting specific aggregation and/or biological properties. The multidisciplinary nature of the gemini surfactant community is exciting and will most likely lead to applications of these surfactants within the fields of biotechnology and biomedicine.

The aim of this review is to cover the aggregation behavior of sugar-based gemini surfactants of the type shown in Figs 1 and 2. These surfactants have been synthesized and characterized in terms of their aggregation behavior in dilute aqueous solution in the research group of one of the authors (J.B.F.N.E.) between 1997 and 2003. The studies have been published in Refs 4–11. For the reader interested in a broader range of gemini surfactants, a number of extensive reviews have recently appeared that cover most aspects of gemini chemistry, including aggregation properties,[2,12–14] synthesis[14] and application within gene therapy.[11]

SUGAR-BASED GEMINI SURFACTANTS

The structure of the sugar-based gemini surfactants is shown in Figs 1 and 2. The synthesis of these surfactants is not the focus of this review and the interested reader

**Correspondence to:* M. Johnsson, Physical Chemistry 1, Chemical Center, Lund University, P.O. Box 124, SE-22100 Lund, Sweden.
E-mail: Markus.Johnsson@fkem1.lu.se
†Paper presented at the 9th European Symposium on Organic Reactivity, 12–17 July 2003, Oslo, Norway.
Contract/grant sponsors: European Commission as part of its Training and Mobility of Researchers (TMR) Programme; The Swedish Foundation for International Cooperation in Research and Higher Education (STINT) (M.J.).

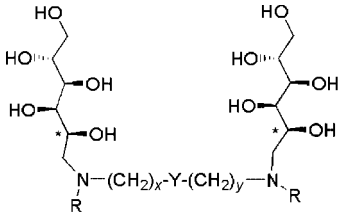

Saturated series, R = C_mH_{2m+1}.

m	*x*	*y*	Y	sugar (reduced)
12	2	2	$(CH_2)_2$	glucose (glu)
14	2	2	$(CH_2)_2$	glu
16	2	2	$(CH_2)_2$	glu
12	1	1	$(CH_2)_2$	glu
14	1	1	$(CH_2)_2$	glu
16	1	1	$(CH_2)_2$	glu

Unsaturated series, R = C18:1 Δ^9 (oleyl).

x	*y*	Y	sugar (reduced)
2	2	$(CH_2)_2$	glu
2	2	$(CH_2)_2$	mannose (man)
2	0	$(OCH_2CH_2)_2$	glu
2	0	$(OCH_2CH_2)_2$	man

Figure 1. Structure of the sugar-based gemini surfactants containing tertiary amines in the headgroup. The difference between glucose (glu) and mannose (man) is the stereochemistry at the carbon atom indicated by the asterix (glu is shown)

may consult some of the original papers for more information on that issue.[4–6,8,9] Instead, we would like to start by highlighting the most important features of the compounds that will ultimately dictate their aggregation behavior. Let us begin with the polar headgroup region and emphasize that the identity of the sugar used in the synthesis can be varied to meet specific requirements. Glucose or mannose have been used in all cases discussed here; however, several other sugars are under consideration and a library of gemini surfactants with different sugar headgroups is therefore under construction. The difference between glucose and mannose is the stereochemistry at the carbon atom indicated with an asterix in Fig. 1. The stereochemistry of the sugar may be important when it comes to a possible targeting of the compounds to

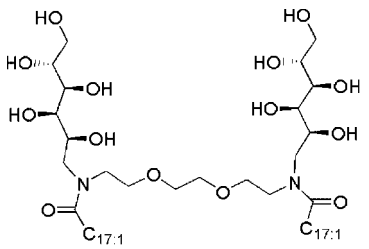

Figure 2. Example of an amide-containing sugar-based gemini surfactant (referred to in the text as 'amide-gemini'). Several other amide-geminis with saturated tails [C(O)—C_mH_{2m+1}, $m = 4$–9, 11, 13, 15] and with aliphatic spacers [—$(CH_2)_n$—, $n = 2$, 4, 6–10, 12] have also been prepared[4,5]

cell surface receptors *in vivo*.[15] Furthermore, different sugars may hydrate differently and this could in turn influence the aggregation behavior in terms of aggregate structure or preferred mean curvature of the surfactant film.

The second feature to be noted is the presence of the two tertiary nitrogens that can be protonated (Fig. 1). Thus, a pH-dependent aggregation behavior is expected. As will be shown and discussed later, protonation of the amines is the decisive parameter as to whether the gemini surfactants will form vesicles or micelles and whether cylindrical or spherical micelles are formed.

The nature of the spacer connecting the two parts of the gemini can, in principle, be varied infinitely and the spacers are usually distinguished by their length, relative polarity and flexibility.[2,12,14] In our case, two different types of spacers have been used, an aliphatic chain of varying length [—$(CH_2)_n$—] or a short ethylene oxide (EO = —OCH_2CH_2—) spacer [—$(CH_2)_2$—$(EO)_2$—] (Figs 1 and 2). Both spacers are flexible but it was expected that the EO spacer would be more hydrophilic than the aliphatic spacer.

Finally, the aliphatic chains or tails have been varied in terms of length, degree of unsaturation and the type of chemical linkage to the headgroup. The nature of the tails has several effects on the physical-chemical behavior of the compounds. The most obvious effect is the modulation of the gel-to-liquid crystalline phase transition temperature of the bilayer in the vesicles formed from the compounds. As with ordinary bilayer-forming phospholipids, the longer the tail the higher the transition temperature.[6] Replacing the saturated tails by unsaturated oleyl tails ($C_{18:1}$) decreases the phase transition temperature considerably and for normal working conditions, i.e. ca 25 °C, the bilayers formed from the oleyl surfactants are in the liquid crystalline phase. The chemical linkage of the tails to the headgroup is also very important. For example, if an amide is present instead of an amine (see Fig. 2), protonation is no longer an issue and the compound in Fig. 2 does not undergo the protonation-driven vesicle-to-micelle transition that is characteristic of the compounds shown in Fig. 1.[9] Several other gemini surfactants of the type shown in Fig. 2 with saturated and shorter hydrocarbon tails and with aliphatic spacers have been prepared and their aggregation properties in aqueous solution characterized.[4,5] Herein we will focus our attention on the type of sugar-based gemini surfactants shown in Fig. 1 and make reference to the type of compounds exemplified in Fig. 2 when appropriate.

AGGREGATION BEHAVIOR: THEORETICAL CONSIDERATIONS

Before reviewing the experimental results for the aggregation behavior of the sugar-based gemini surfactants it is useful to consider briefly some predictions from conventional theory on surfactant aggregation. A popular

Table 1. Relationship between molecular shape, packing parameter and preferred aggregate structure

Molecular shape	P	Aggregate structure
Cone	$\leq 1/3$	Spherical micelles
Truncated cone	$1/3 < P \leq 1/2$	Cylindrical micelles
Truncated cone	$1/2 < P < 1$	Flexible bilayers, vesicles
Cylinder	≈ 1	Planar bilayers
Inverted truncated cone	>1	Inverted micelles

approach used to predict the aggregate structure is based on a knowledge of the molecular geometry or shape of the surfactant molecule.[16] The basic idea is that for every type of surfactant, there exists an optimal interfacial headgroup area, a_0, at which the Gibbs energy of the surfactant in the aggregate is minimized.[16] A shape factor or packing parameter, P, is defined as:

$$P = V/(a_0 \times l_c) \quad (1)$$

where V is the hydrophobic chain volume and l_c is the critical length of the hydrophobic chain (or chains). Based on the magnitude of this simple packing parameter, the structure of the aggregates that are formed can be predicted. Thus, the following aggregate morphologies are expected as P is varied from $\leq 1/3$ to >1 (Table 1).

Some of the aggregates indicated in Table 1 are schematically depicted in Plate 2.

It is worth mentioning that the packing parameter does not furnish a unique description of surfactant aggregation because there are several types of aggregates other than those indicated in Table 1 that may occur in surfactant systems. For example, dispersed mesh-like as well as disk-like structures have been detected in several lipid–surfactant–water systems[17,18] where the individual values of the lipid and surfactant packing parameters are of little guidance. Furthermore, the interfacial headgroup area often depends strongly on the solution conditions, meaning that parameters such as pH, ionic strength and temperature have to be specified for a given packing parameter for it to be useful. It is also important to note that the packing parameter is not as easily applied for gemini surfactants as it is for most single-tailed conventional surfactants or double-tailed conventional phospholipids. The reason is that the headgroup of the geminis is not free to find its equilibrium area in a thermodynamic sense, because of the constraints of the spacer connection between the two surfactant parts. In fact, it has been found that the distribution of distances between gemini headgroups is bimodal, with a maximum at the thermodynamic equilibrium distance and another maximum that corresponds to the 'spacer-induced' distance, which is characterized by the length and rigidity of the spacer.[2] On the other hand, the two maxima tend to coincide for flexible spacers of sufficient length and in these cases the packing parameter concept then becomes more useful.

We now proceed to the consideration of what the possible values of the packing parameter would be for our sugar-based gemini surfactants. Let us take a closer look at the compounds shown in Fig. 1. First of all, the surfactants have two hydrocarbon tails and V is therefore rather large. It is also possible that the spacer will contribute to the hydrophobic volume. A large V will tend to increase P. On the other hand, V and l_c are not independent and a large V means a large l_c which will tend to lower P. The decisive parameter will be the optimal interfacial headgroup area and because the surfactants have titratable tertiary amines in the headgroup, the pH will be very important. Let us assume that the molecular shape of the *monoprotonated* surfactant, independent of the values of m, x, y and Y and the degree of unsaturation (Fig. 1), can be approximated as a truncated cone or cylinder, characterized by $1/2 < P \leq 1$. This is reasonable if one compares the monoprotonated gemini with typical double-tailed bilayer-forming phospholipids, such as egg lecithin (egg phosphatidyl choline) or phosphatidyl glycerols.[19] With this assumption we expect the formation of lamellar aggregates, such as vesicles for the monoprotonated geminis dispersed in aqueous solution. As the pH is lowered, more of the geminis will become doubly protonated and a_0 will increase due to increased electrostatic repulsion between the headgroups. Accordingly, P will decrease, predicting the formation of micellar aggregates (Table 1, Plate 2). If the ideal sequence indicated in Table 1 is followed, we expect that the first micellar aggregates to appear will be cylindrical micelles. Finally, at full protonation (low pH), we expect the formation of spherical micelles in analogy with comparable ammonium gemini surfactants.[2] It should be noted that the spacers used are comparably long and always of the flexible type (Fig. 1). Therefore, the use of the packing parameter concept seems valid, although it does not predict the exact pH at which the structural transition takes place. Furthermore, structures other than those given in Table 1 may well occur and only experiment can tell the full story.

Finally, the 'amide-gemini' shown in Fig. 2 does not possess any obvious titratable sites (at least not for $pH < 11$) and being a double-tailed $C_{18:1}$-surfactant with a relatively large headgroup, we may approximate the molecular shape as a truncated cone or cylinder. Accordingly, over a large pH interval, this surfactant is expected to form bilayer structures such as vesicles.

AGGREGATION BEHAVIOR: EXPERIMENTAL RESULTS

The following sections deal with experimental results obtained from dilute aqueous solutions of the compounds shown in Figs 1 and 2.[4–9] The amphiphile concentration has in general been ≤ 1 wt% and the compounds have been dispersed in pure water or in a 15 mM electrolyte

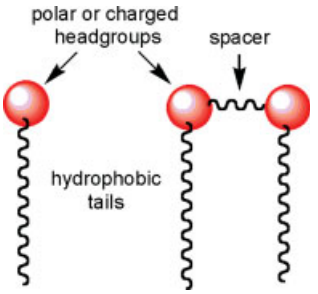

Plate 1. Schematic drawing of a conventional (left) and gemini surfactant (right)

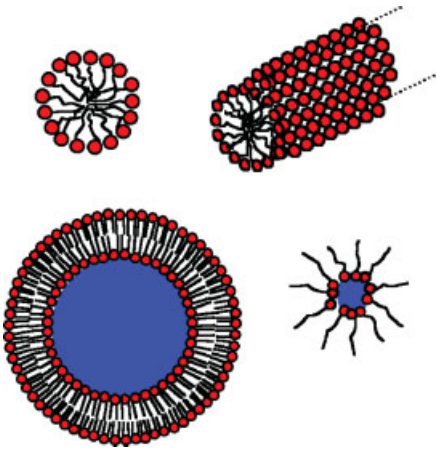

Plate 2. Schematic cross-sectional views of a spherical micelle (top, left), cylindrical micelle (top, right), vesicle containing an aqueous core (blue color) (bottom, left) and an inverted spherical micelle containing an aqueous core (blue color) (bottom, right)

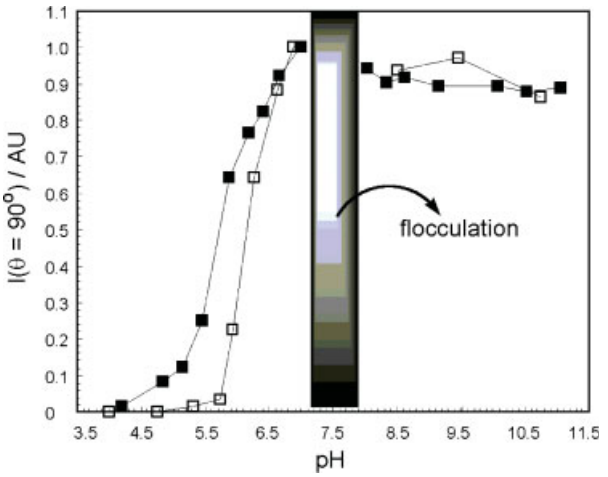

Plate 3. Scattering intensity measured at an angle of 90° as a function of solution pH. The surfactant concentration was 0.5 mM and the results displayed pertain to gemini surfactants with $R = C_{18:1}$ and (□) $x = y = 2$, $Y = (CH_2)_2$, man; (■) $x = 2$, $y = 0$, $Y = (OCH_2CH_2)_2$, man. Gray area indicates the pH region of colloidal instability (flocculation). Reprinted with permission from Ref. 9 Copyright (2003) American Chemical Society

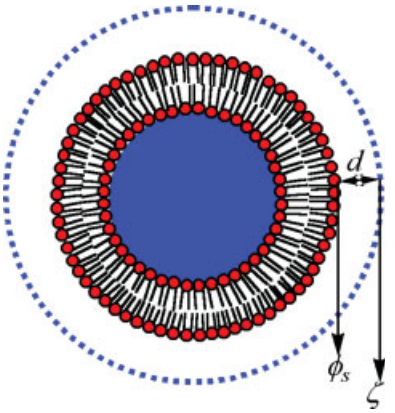

Plate 4. Schematic representation of the location of the shear plane where the ζ-potential is estimated from electrophoretic mobility measurements. The distance d is generally around a few Ångströms. ϕ_s is the surface potential

(buffer or NaCl) solution. The preparation of the samples has, however, varied somewhat, depending on the purpose and type of gemini; the procedure typically involves brief ultrasound treatment (sonication) to obtain coarsely dispersed mixtures, followed by further refinements such as freeze–thaw treatment and extrusion through polycarbonate filters of well-defined pore size. The majority of the samples have been prepared at pH ca 7 and the pH is then adjusted as required with small aliquots of aqueous HCl or NaOH. Most of the measurements were conducted at 25 °C.

Aggregate size triggered by changes in solution pH

A simple and straightforward way to obtain an overview of the aggregation behavior of the compounds shown in Fig. 1 is to measure the scattered light intensity of the aqueous dispersions as a function of the solution pH.[8,9] Vesicular dispersions appear turbid or bluish due to light scattering whereas micellar samples are transparent and thus scatter much less light. Accordingly, it is possible to identify the approximate pH values where micelle formation or other structural transitions take place by measuring the scattered light intensity.

Plate 3 displays a typical result of a light scattering experiment from dispersions containing 0.5 mM of gemini surfactant (Fig. 1). The compounds were dispersed in a 15 mM buffer solution at pH ca 7 using brief sonication followed by repeated freeze–thaw (liquid N_2 $\leftrightarrow$ waterbath, 50 °C) cycles and the samples were finally extruded through 200 nm pore-sized polycarbonate filters.[9] This procedure produced turbid to bluish dispersions indicating the presence of large aggregates in the samples. Indeed, as shown in Plate 3, the scattered light intensity reached maximum values above pH 6.5. As will be shown later, large unilamellar vesicles are the reason for this observation. When the pH is lowered below pH 6, the intensity drops considerably indicating the disappearance of the vesicles and the formation of other aggregates. Below pH 5.5, the scattered light intensity is low in both the displayed cases and the solutions appear optically clear. The transparent solutions indicate the transition from vesicular to micellar aggregates. It should be emphasized that very similar results have been obtained for all of the compounds indicated in Fig. 1, the only differences being the exact pH values at which the intensity (or turbidity) starts to drop.[6–9] We may also add that another way of following changes of the aggregation/protonation state of the geminis is to measure the surface tension of the dispersions as a function of pH.[6,7] As the pH is lowered, the monomer activity increases due to the formation of divalent (doubly protonated) surfactants and the surface tension versus pH profiles correlate well with the intensity or turbidity versus pH profiles.

Another very interesting observation in these systems is the colloidal instability of the vesicles in a certain pH interval. For the geminis investigated in Plate 3, this instability is observed around pH 7.5 ($\pm$0.3) and is indicated by the shaded region.[9] Around pH 7.5, the vesicles flocculate (aggregate) rapidly (within seconds) and a sedimentation of large particles can be visually observed after a few minutes. Somewhat surprisingly, the sedimented large particles could be easily redispersed by raising the pH slightly and with gentle magnetic stirring of the solutions. As shown in Plate 3, the scattered light intensity remains essentially at the same value after redispersal indicating that there is no aggregate growth that would otherwise have resulted in higher intensity readings. Again it should be noted that similar results have been obtained for most of the compounds shown in Fig. 1. We will discuss the observed phenomena in more detail in the sections to come.

Finally, for the compound shown in Fig. 2, there was very little change of the scattered light intensity with pH.[9] The dispersion of the 'amide-gemini' appeared turbid to bluish indicating the presence of large particles (vesicles) over the whole pH interval. However, also in this case we observed a colloidal instability of the vesicles when the pH was lowered to pH ca 5.[9] Extensive flocculation was observed but as discussed above, the large sedimented aggregates could easily be redispersed by titrating the sample back to higher pH with concomitant magnetic stirring. In this respect it should be noted that 'amide-geminis' with shorter hydrocarbon tails [C(O)—$C_{13}H_{27}$] display a more complex aggregation behavior than is apparent for the compound in Fig. 2.[4] In fact, depending on the spacer length [—$(CH_2)_n$—, $n = 6, 8, 10$] and on the temperature, these surfactants form either cylindrical micelles or vesicles.[4] In relation to the packing parameter (Table 1), this indicates that small variations in the gemini structure or temperature 'push' P in either direction of the vesicle/cylindrical micelle 'boundary', that is, the P value is close to 0.5. It is worth noting that the compound with $n = 10$ formed vesicles at all temperatures investigated[4] supporting the idea that the spacer volume should be taken into account in the estimation of the hydrophobic volume (V) [Eqn (1)].

Vesicle-to-micelle transition followed by dynamic light scattering (DLS) and cryo-transmission electron microscopy (cryo-TEM)

The data presented in Plate 3 support the protonation-driven vesicle-to-micelle transition. However, to gain more quantitative insights we require more sophisticated methods to study the process. In Fig. 3, we present dynamic light scattering (DLS) data obtained from samples containing the gemini surfactant with $R = C_{18:1}$, $x = 2$, $y = 0$, $Y = (OCH_2CH_2)_2$ and reduced mannose as the polar headgroup (Fig. 1).[9] It is clear that the mean

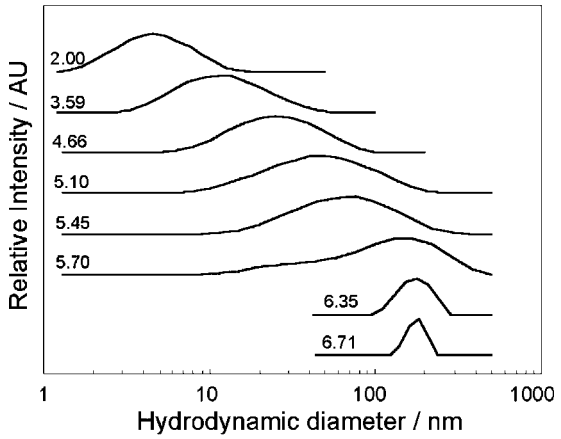

Figure 3. Size-distributions obtained using DLS from a sample containing the gemini surfactant with $R = C_{18:1}$ and $x = 2$, $y = 0$, $Y = (OCH_2CH_2)_2$, man. The solution pH is indicated next to the respective size distribution. Reprinted with permission from Ref. 9 Copyright (2003) American Chemical Society

apparent diameter of the aggregates decreases from ca 180 nm at pH 6.7 to ca 5 nm at pH 2. Furthermore, in the pH interval between these values, relatively broad size distributions are obtained and the mean intensity-averaged diameter decreases in a continuous fashion as the pH is lowered. Interestingly, the pH of ca 5.7, where the aggregates give rise to the broad size distribution, appears to correlate with the dramatic drop in the intensity readings (Plate 3) and also with a significant viscosity increase. The latter effect is especially pronounced at surfactant concentrations ≥ 5 mM (≈ 0.5 wt%). These results can be rationalized if we take into account that samples containing cylindrical or worm-like micelles are often more viscous than vesicle dispersions.

Thus, the picture that emerges for this particular sugar-based gemini surfactant is of a vesicle-to-micelle transition at pH ≈ 5.7 and the first micellar structures to appear in the samples are cylindrical micelles. Whereas similar results have been obtained for all the sugar-based geminis in the unsaturated series[8,9] (Fig. 1), the process remains to be studied in detail for the saturated series (Fig. 1). We would also like to add that angle-dependent intensity light scattering measurements support the DLS-data on the vesicle-to-cylindrical micelle transition (not shown).[8,9] Note also that the hydrodynamic diameter at pH 2 is only about 5 nm, consistent with the formation of small spherical or globular micelles for the divalent cationic amphiphiles.

Cryo-transmission electron microscopy (cryo-TEM) provides a unique means of studying self-assembled aggregates in dilute aqueous solution.[20,21] A thin film of the surfactant–water dispersion is formed by a blotting procedure where excess solution is removed from the electron microscopy grid (EM-grid) by means of a filter paper. The resulting film, approximately 0.5 μm thick, is then rapidly plunged into liquid ethane for vitrification. The film is vitrified in ≤ 0.1 ms which assures a minimum of sample perturbation and the vitrification enables visualization of the surfactant aggregates present in the sample.[20,21] Combined with techniques that give better statistics, such as DLS, a very good picture of the samples can be obtained. The cryo-TEM micrographs displayed in Fig. 4 were obtained from samples containing the gemini surfactant with $R = C_{18:1}$, $x = 2$, $y = 2$, $Y = (CH_2)_2$ and reduced mannose as polar headgroup (Fig. 1).[9] Clearly, the cryo-TEM results support the picture obtained from DLS, that is, vesicles are formed close to neutral pH whereas cylindrical micelles are formed at intermediate pH. Note that the bilayer structure of the vesicles is resolved and that the estimated bilayer thickness is ≈ 4 nm, a value that is reasonable for a bilayer consisting of surfactants with oleyl ($C_{18:1}$) tails.[22] Note also that coexistence between relatively short cylindrical micelles and small spherical micelles can be observed at pH 4.7. The small globular micelles are observed as small dark dots in the cryo-TEM micrograph. This coexistence was not resolved in the DLS measurements (Fig. 3) since a bimodal size distribution should have been observed, whereas a broad monomodal distribution was obtained. Nevertheless, the agreement between DLS and cryo-TEM is good corroboration for the 'ideal behavior' of these systems according to the packing parameter concept (Table 1). In this context we may also add that the small micelles (diameter ≈ 5 nm) observed using both cryo-TEM and DLS were further investigated using steady-state fluorescence quenching (SSFQ) measurements.[9] The micelle aggregation number was found to be between 15 and 20 at pH 2, in good agreement with geometric estimations based on the results from cryo-TEM and DLS.[9]

Another question that can be resolved using cryo-TEM is how the cylindrical micelles actually form from the original vesicle dispersion. Figure 5 is obtained at pH ≈ 6 from the gemini surfactant with $R = C_{18:1}$, $x = 2$, $y = 0$, $Y = (OCH_2CH_2)_2$ and reduced glucose as the polar headgroup (Fig. 1). Clearly, cylinders can be observed to grow directly from the vesicle bilayers. Accordingly, there is a narrow pH interval where bilayer structures and cylindrical micelles coexist and this coexistence may, at least on the time-scale investigated (≤ 24 h), occur within one single aggregate.

Characterization of the gemini vesicles

Having thoroughly established the vesicle-to-micelle transition with several different techniques, we now turn our attention to the vesicular pH region. Let us start by the preparation of the vesicles. In general, vesicles are formed from all of the compounds in Fig. 1 around neutral pH.[6–9] In addition, the amide-gemini shown in Fig. 2 forms vesicles at all relevant pH values.[9] In several of the previous publications, the compounds have simply

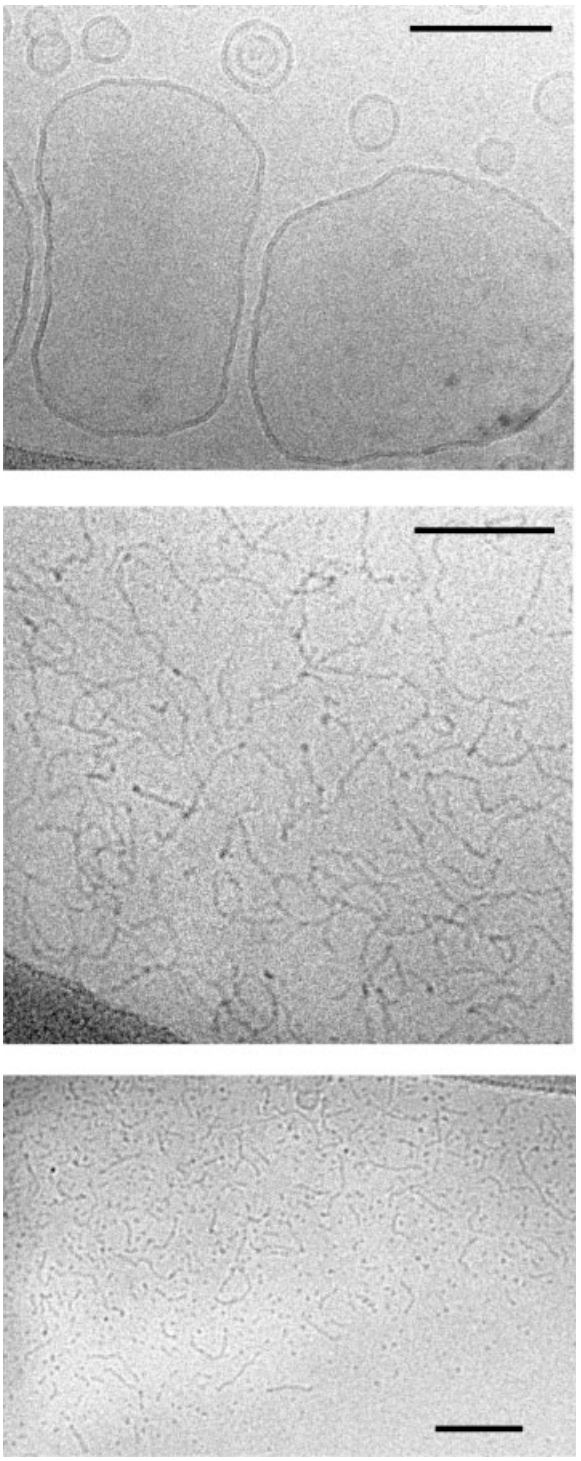

Figure 4. Cryo-TEM images of samples containing the gemini surfactant (5 mM) with $R = C_{18:1}$, $x = 2$, $y = 2$, $Y = (CH_2)_2$, man. The solution pH was 7.1 (top), 5.4 (middle) and 4.7 (bottom). Note the small globular micelles, observed as small dark dots, coexisting with relatively short cylindrical micelles in the bottom part. Scale bar = 100 nm. Reprinted with permission from Ref. 9 Copyright (2003) American Chemical Society

been dispersed in aqueous solution by sonication.[6,7] This often produced complex multimodal or bimodal size distributions, as detected by DLS.[6] Because it is often an advantage to work with vesicles of fairly narrow size

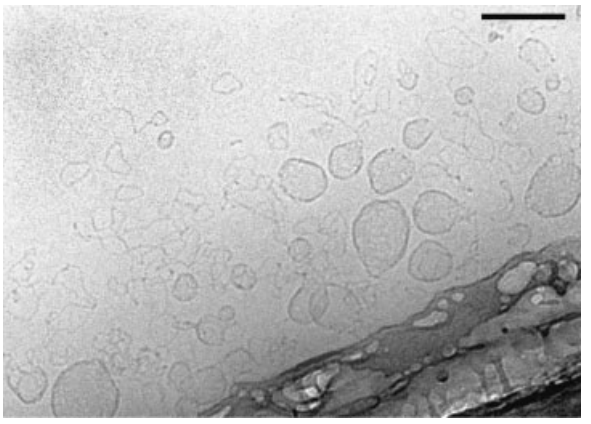

Figure 5. Cryo-TEM image obtained at pH ≈ 6 from the gemini surfactant (5 mM) with $R = C_{18:1}$, $x = 2$, $y = 0$, $Y = (OCH_2CH_2)_2$, glu. Note cylinders growing out from defect vesicles. Scale bar = 100 nm

distributions and reproducible mean sizes, we have in later publications[8,9] further refined the sonicated dispersions by employing freeze–thaw cycles and thereafter extrusion through polycarbonate filters with pore-sizes of 200 nm. As shown in Fig. 6, this procedure yielded well-defined vesicle dispersions with the mean vesicle size being 180 ± 20 nm.

In the case of the saturated gemini series (Fig. 1), it is highly relevant to determine the bilayer gel-to-liquid crystalline phase transition temperature, T_m. This temperature is conveniently determined using differential scanning calorimetry (DSC). For normal double-tailed phospholipids, T_m is an increasing function of the tail-length[23] and the saturated geminis displayed the same trends as shown in Fig. 7.[6] The dependence of T_m on the length of the spacer was found to be less significant.[6] The T_m is of great importance when it comes to a possible application of these gemini surfactants in, for example, DNA delivery, because it is often required that the bilayer resides in the liquid crystalline phase for optimal performance.[10,11] As previously stated, all the geminis in the

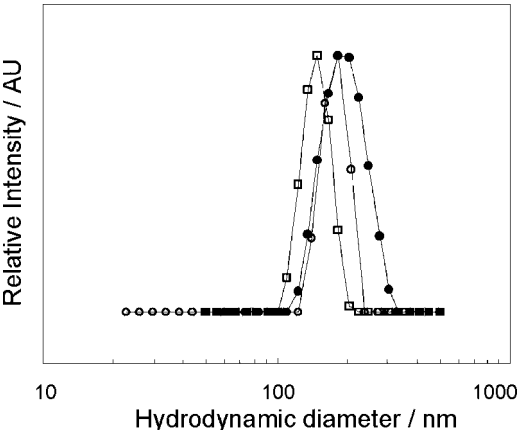

Figure 6. Size distributions of extruded vesicles made from gemini surfactants with $R = C_{18:1}$ and (□) $x = 2$, $y = 0$, $Y = (OCH_2CH_2)_2$, glu; (○) $x = 2$, $y = 0$, $Y = (OCH_2CH_2)_2$, man and (●) the amide-gemini, glu (Fig. 2)

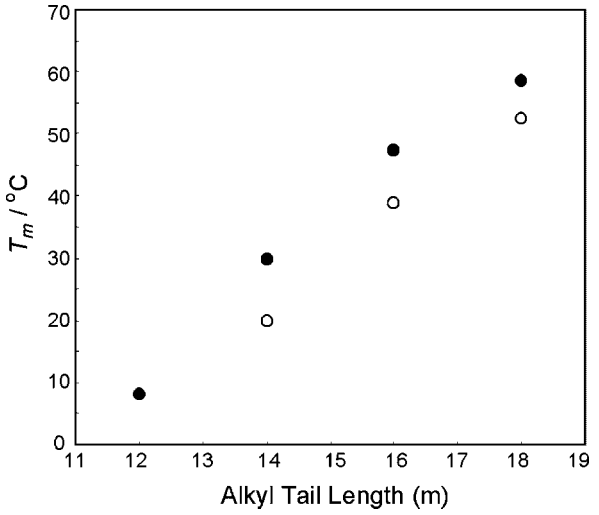

Figure 7. Phase transition temperature (T_m) as a function of alkyl tail length (m) of bilayer vesicles formed from the saturated series (Fig. 1). (○) $x=2$, $y=2$, $Y=(CH_2)_2$, glu; (●) $x=2$, $y=0$, $Y=(CH_2)_2$, glu. Reprinted with permission from Ref. 6 Copyright (2001) FEBS

unsaturated series (Fig. 1) exhibit a T_m well below room temperature, most probably below 0 °C.[6]

We now turn to the intriguing phenomenon displayed in Plate 3, that is, the flocculation of the vesicles and the redispersal after a small increase in the hydroxide ion concentration. First of all it should be emphasized that the flocculation–redispersal process was found to be completely reversible and that the mean size of the redispersed vesicles was the same as before flocculation.[8,9] This led us to believe that the large aggregates (floccs) observed in the relevant pH regions must consist of loosely bound but individually intact vesicles. Indeed, cryo-TEM confirmed our hypothesis as shown in Fig. 8. This image was recorded from a sample containing vesicles formed from the gemini with $R=C_{18:1}$, $x=2$, $y=0$, $Y=(OCH_2CH_2)_2$ and reduced glucose as the polar headgroup. The vesicles were made to flocculate by raising the pH from 6.7 to a pH within the colloidal instability region, pH ≈ 7.4.[9] Clearly, the vesicles are aggregated in a fashion that supports the view of individually intact vesicles. Cryo-TEM images of the sample after redispersal confirmed the presence of vesicles also at higher pH (not shown).

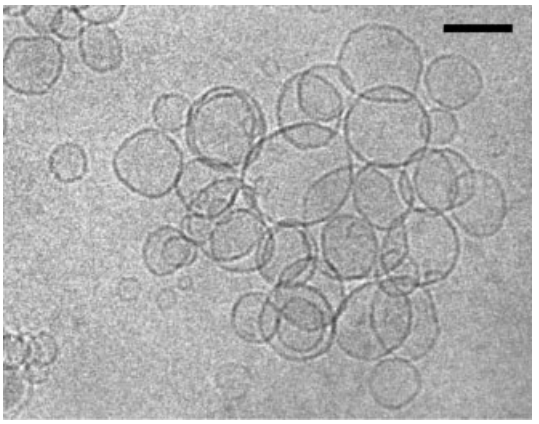

Figure 8. Cryo-TEM image of flocculated vesicles made from the gemini (5 mM) with $x=2$, $y=0$, $Y=(OCH_2CH_2)_2$, glu. The vesicles were flocculated by raising the solution pH from pH 6.7 to 7.4. The sample was vitrified 1 min after the onset of flocculation. Scale bar = 100 nm. Reprinted with permission from Ref. 9 Copyright (2003) American Chemical Society

Having established that the morphology of the vesicles was unaffected by the flocculation–redispersal process, we examined the mechanism behind this phenomenon. Because colloidal particles, such as vesicles, often owe their colloidal stability in aqueous solution to repulsive long-ranged electrostatic interactions,[24] a good starting point for the investigation would be to measure the surface potential (ϕ_s) or rather the more accessible zeta potential (ζ-potential) as a function of pH. The ζ-potential was determined from electrophoretic mobility measurements and essentially reports the electrostatic potential of the vesicles at the shear or slipping plane.[24,25] The shear plane is located at a small (unknown) distance (d) from the surface as shown in Plate 4.

Despite being a somewhat vague concept due to the problem of defining the location of the shear plane, it has been shown that the ζ-potential gives a good indication of the magnitude of the repulsive electrostatic interaction between the particles.[24–26] According to the classical DLVO-theory on colloidal stability,[24] attractive van der Waals (vdW) interactions and repulsive electrostatic interactions determine the colloidal stability of the particles. Accordingly, when the ζ-potential is small one expects colloidal instability due to a dominance of the attractive vdW interactions. In this respect it should be noted that the DLVO-theory is in general not sufficient to describe the interactions between fluid amphiphilic bilayers or vesicles.[27] The reason is that short-range repulsive steric entropic interactions as well as so-called hydration forces usually also confer colloidal stability to uncharged particles/vesicles.[27,28] Nevertheless, we may, as a starting point, consider the predictions from the DLVO-theory as a semi-quantitative guideline for the behavior of the systems.

In Fig. 9 we have plotted typical ζ-potential versus pH profiles of vesicles formed from two of the geminis,[9] including the amide-gemini (Fig. 2). Several interesting conclusions may be drawn from these results. Firstly, the pH region of colloidal instability for the respective gemini surfactant vesicles correlates very well with low ζ-potentials. This is in accordance with the DLVO-theory as discussed above. Secondly, for the gemini with $R=C_{18:1}$, $x=2$, $y=0$, $Y=(OCH_2CH_2)_2$ and glucose as the polar headgroup, the vesicles exhibit a charge reversal, going from cationic to anionic vesicles above pH 7.1. Thirdly, despite being a neutral surfactant with no obvious titratable sites in the investigated pH region, the vesicles formed from the amide-gemini (Fig. 2) exhibit negative ζ-potentials above pH ca 5.

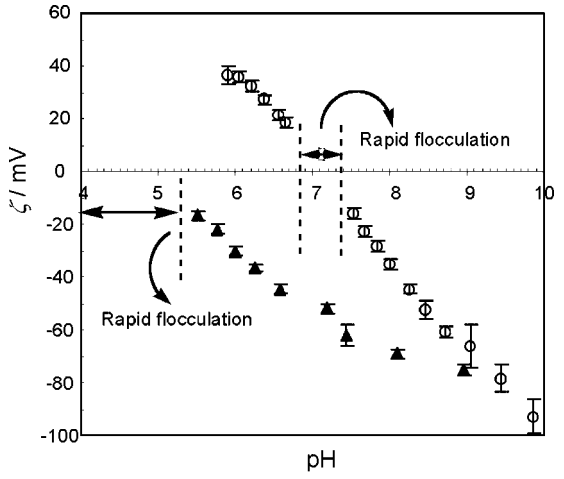

Figure 9. ζ-potential of vesicles made from the gemini surfactants with (○) $R = C_{18:1}$, $x = 2$, $y = 0$, $Y = (OCH_2CH_2)_2$, glu and (▲) the amide-gemini (Fig. 2). The colloidal instability regions are indicated in the figure and in both cases the instability was observed when $\zeta \leq |15\ mV|$. The ionic strength of the solutions was approximately 15 mM (15 mM buffer). Reprinted with permission from Ref. 9 Copyright (2003) American Chemical Society

It appears clear from Fig. 9 that the surface charge of the vesicles can explain the flocculation–redispersal phenomenon displayed in Plate 3, that is, the negative ζ-potential at pH >7.4 is high enough to explain the reoccurring colloidal stability in terms of repulsive electrostatic interactions.[8,9] Similarly, for the amide-gemini, the negative surface charge, or ζ-potential, is low below pH 5.5 explaining the flocculation of these vesicles in this pH region. Again we would like to emphasize that this discussion is based on the predictions of the DLVO-theory and that short-range attractive or repulsive interactions have been ignored. Attractive short-range interactions may result from inter-vesicular hydrogen bonding in the present systems, similar to what has been observed between glycine-based amphiphile bilayers.[29]

The question that now arises concerns the charging mechanism. For the compounds shown in Fig. 1 it is obvious that one should expect cationic vesicles due to protonation but it is more difficult to understand the negative surface charge. Similarly, what mechanism is responsible for the negative surface charge of the vesicles formed from the compound in Fig. 2? We may consider two different mechanisms for the negative surface charge: (*i*) a deprotonation of the sugar hydroxyl groups leading to negatively charged sugar headgroups or (*ii*) adsorption of negative ions from bulk solution onto the vesicle surface.

In general, the pK_a of sugar hydroxyl groups is in the order of 12–13,[30] which appears to be too high to explain the negative surface charge in the present cases. On the other hand, protonation of the amines (Fig. 1) may render the sugar hydroxyl groups more acidic than what is normally the case. However, protonation is not an issue in the case of the amide-gemini and, consequently, protonated amines cannot explain an abnormally low sugar hydroxyl pK_a.

The second mechanism (*ii*) requires the adsorption of negative ions onto the vesicle surface. This charging mechanism is well-known from a variety of colloidal systems and it is often found that ion-adsorption follows the so-called Hofmeister series.[31–33] The Hofmeister series can be illustrated by taking the halide ions as an example where *non-specific* adsorption to surfaces increases in the order $Cl^- < Br^- < I^-$. There is thus a correlation between ion polarizability and adsorption propensity. The problem in our case is that we have used both buffer solutions and NaCl solutions and obtained essentially identical ζ-potential versus pH profiles[8,9] and we therefore discarded a 'Hofmeister-type' of mechanism. The only other negative ions, besides Cl^- or buffer species, present in bulk solution are hydroxide ions (OH^-). Hydroxide ions are known to adsorb onto oil-droplets and onto a variety of surfactant-covered interfaces.[34–38] Interestingly, it has been argued that OH^- adsorbs onto vesicles formed from glycolipids[30,39] resulting in negatively charged vesicles. This observation seems particularly relevant in the case of the sugar-based gemini surfactants. Moreover, the colloidal stability of vesicles of plant thylakoid galactolipids, such as digalactosyl-diacylglycerol (DGDG), has been shown to be extremely sensitive to the electrolyte concentration.[40,41] Thus, seemingly neutral glyco- or galactolipid vesicles behave as though they were composed of charged lipids.

Whatever the true mechanism of the negative charging of the vesicles, we can set up a number of surface equilibrium reactions that may occur for the gemini vesicles (Scheme 1):

In Scheme 1, N(1), N(2), S—OH and S are the respective binding or dissociation sites on the surfactant headgroup or at the vesicle surface and K_1, K_2, K_a and K_{OH} are the equilibrium constants associated with each binding/dissociation site. Equations (2)–(5) pertain to the geminis in Fig. 1 whereas only Eqns (4) and (5) are relevant for the amide-gemini (Fig. 1). Note that depending on the mechanism [(*i*) or (*ii*)], either Eqn 4 (*i*) or Eqn 5 (*ii*) is appropriate. Before outlining the theoretical model of the ζ-potential versus pH profiles, it should be noted that in Refs 8 and 9 we decided on the hydroxide ion

$$N(1) + H^+_{surf} \overset{K_1}{\rightleftharpoons} N(1)H^+ \quad (2)$$

$$N(2) + H^+_{surf} \overset{K_2}{\rightleftharpoons} N(2)H^+ \quad (3)$$

$$S{-}OH \overset{K_a}{\rightleftharpoons} S{-}O^- + H^+_{surf} \quad (4)$$

$$S + OH^-_{surf} \overset{K_{OH}}{\rightleftharpoons} SOH^- \quad (5)$$

Scheme 1

binding-mechanism (*ii*). Unfortunately, the model that will be presented does not discriminate between the mechanisms and identical theoretical results are obtained employing the dissociation mechanism [(*i*), Eqn (4)]. This is important to keep in mind during the presentation of the model below. Thus, the following section is based on the choice of the binding mechanism (*ii*) but we will comment on the possibility of dissociation mechanism (*i*) later on.

The degree of binding (f) to the respective binding site can be determined according to Eqns (6) and (7):

$$f_{N(i)} = \frac{K_i[H^+]_{bulk}\exp\left(\frac{-e\phi_s}{k_BT}\right)}{1 + K_i[H^+]_{bulk}\exp\left(\frac{-e\phi_s}{k_BT}\right)}; i = 1,2 \qquad (6)$$

$$f_s = \frac{K_{OH}[OH^-]_{bulk}\exp\left(\frac{e\phi_s}{k_BT}\right)}{1 + K_{OH}[OH^-]_{bulk}\exp\left(\frac{e\phi_s}{k_BT}\right)} \qquad (7)$$

In Eqns (6) and (7), e is the elementary charge and k_BT is the Boltzmann temperature. From f we can calculate the vesicle surface charge density σ according to Eqns (8) and (9), where only Eqn (9) is relevant for the amide-gemini:

$$\sigma = \frac{e}{a_{site}}\left[f_{N(1)} + f_{N(2)} - f_s\right] \qquad (8)$$

$$\sigma = \frac{-e}{a_{site}} f_s \qquad (9)$$

Here, a_{site} is the binding site area for protons and hydroxide ions. To quantify the binding constants, we need to be able to reproduce theoretically the ζ-potential versus pH profiles using a model for the electrostatics in the systems. Previously[8,9] we employed a Poisson–Boltzmann (PB) model[42] for this purpose whereby ϕ_s could be calculated for a given surface charge density. The surface potential was calculated from the Poisson-Boltzmann equation in the spherical symmetry using the computer program PBCell.[43] The binding site area was assumed to be 110 Å^2 in the case of the compounds in Fig. 1 whereas a_{site} was treated as a fitting parameter in the case of the amide-gemini (Fig. 2). We also assumed that the shear plane (Plate 4) was located 5 Å out from the charge plane such that $\zeta \equiv \phi(d = 5\text{ Å})$. With these assumptions we varied the values of the binding constants until the best agreement between the experimentally and calculated ζ-potential versus pH profiles was obtained.

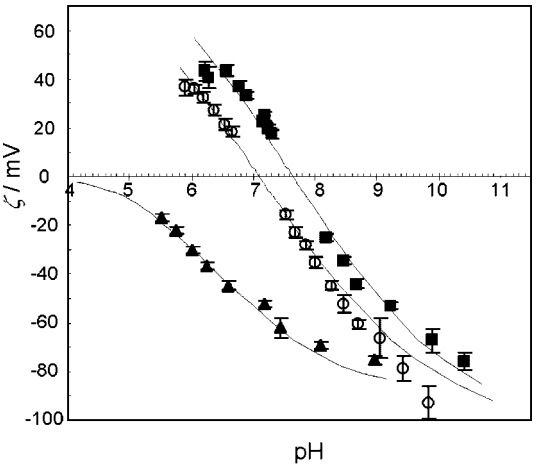

Figure 10. ζ-potential of vesicles made from the gemini surfactants with R = $C_{18:1}$ and (○), $x = 2$, $y = 0$, Y = $(OCH_2CH_2)_2$, glu, (■) $x = 2$, $y = 2$, Y = $(CH_2)_2$, man and (▲) the amide-gemini (Fig. 2). Fully drawn lines represent the PB-model calculations (see text). Reprinted with permission from Ref. 9 Copyright (2003) American Chemical Society

For the interested reader a more detailed description of the modelling can be found in Refs 8 and 9. Some of the fitted curves are shown in Fig. 10.

As is evident from Fig. 10, the PB-model successfully reproduces the experimentally determined ζ-potential versus pH profiles indicating that the approach using surface equilibrium reactions in combination with a PB-model is appropriate. As an example of the information obtained from the fits, the results for the geminis investigated in Fig. 10 are displayed in Table 2.

It is clear that K_{OH} is very high, corresponding to Gibbs binding energies (ΔG^0_{OH}) for OH^- binding of around -18 (± 2) *RT*. The Gibbs binding energies obtained are in good agreement with previously published values of OH^- adsorption onto oil-droplets[34] or glycolipid vesicles.[30] However, the OH^- binding site area of 110–200 Å^2 is about 10 times smaller than what was found for OH^- adsorption in the case of the oil-droplets[34] and the glycolipid vesicles.[30]

Clearly it is difficult to pinpoint the exact driving force that could result in such high levels of hydroxide binding. The question therefore remains open as to whether the negative surface charge of these sugar-based gemini surfactant vesicles is due to dissociation or adsorption [Eqn (4) versus Eqn (5)]. In this respect it is interesting to estimate what the pK_a of the sugar-hydroxyl groups [Eqn (4)] must be in order to explain the results shown in Fig. 10. With pK_a values of 6–7, good fits to the

Table 2. Parameters obtained from the PB-model calculations

Entry[a]	Isoelectric point	log K_1	log K_2	log K_{OH}	a_{site}/Å^2	$\Delta G^0_{OH}/RT$
1	pH = 7.10	8.1	6.0	8.65	110	−19.9
2	pH = 7.65	8.5	5.8	7.30	110	−16.8
3	pH ~ 4.0			7.85	200	−18.1

[a] **1**, R = $C_{18:1}$, $x = 2$, $y = 0$, Y = $(OCH_2CH_2)_2$, glu; **2**, R = $C_{18:1}$, $x = 2$, $y = 2$, Y = $(CH_2)_2$, man; **3**, amide-gemini (Fig. 2).

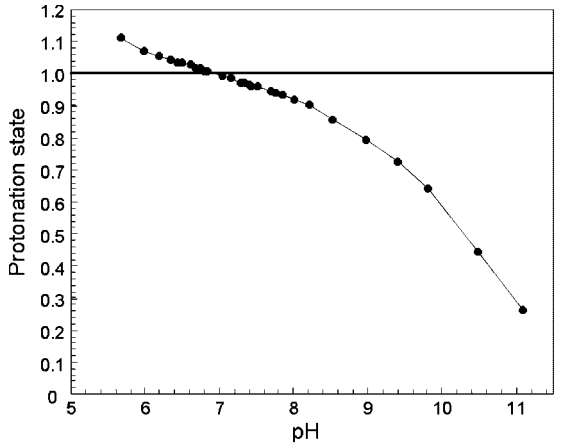

Figure 11. Protonation state as a function of pH of the gemini surfactant with with $R = C_{18:1}$, $x = 2$, $y = 0$, $Y = (OCH_2CH_2)_2$, glu. The results were obtained using the PB-model (see text). The calculations pertain to the vesicular aggregation state. Note that cylindrical micelles are formed in this system below pH 6 (±0.1)

experimental data are obtained (not shown). This appears somewhat unrealistic considering that the pK_a of sugar hydroxyl groups is normally in the range of 12–13.[30] Nevertheless, we cannot completely rule out the 'dissociation-mechanism' and more experiments are needed to clarify this issue.

Characterization of gemini protonation state as a function of pH

A very useful property of the proposed PB-model is that we can calculate the protonation state of the amine-containing geminis as a function of pH. An example of such a calculation is shown in Fig. 11 for the gemini with $R = C_{18:1}$, $x = 2$, $y = 0$, $Y = (OCH_2CH_2)_2$ and glucose as the polar headgroup.

This gemini surfactant forms cylindrical micelles[8] below pH 6 and as can be seen in Fig. 11, the calculated protonation degree is about 1.1 at this pH. Thus, only about 10% of the gemini molecules in the vesicle bilayer are *doubly* protonated when cylindrical micelle formation occurs. For comparison, we have estimated the packing parameter of the monoprotonated (P_{1+}) and doubly protonated (P_{2+}) gemini surfactant to be 0.55 and 0.33, respectively.[9] Using the packing parameter concept (Table 1) as in Eqn (10) the predicted fraction of *doubly* protonated gemini (X_{2+}) at the onset of cylindrical micelle formation becomes 0.23 (23%).

$$X_{1+}P_{1+} + X_{2+}P_{2+} = (1 - X_{2+})0.55 + X_{2+}0.33 = 0.5 \quad (10)$$

Thus, the agreement between the PB-model calculations and the predictions from conventional surfactant aggregation theory is relatively good. In any case it is clear that only a small fraction of the gemini surfactants needs to be doubly protonated for the cylindrical geometry (micelles) to be the preferred aggregate geometry. In addition, as the pH is lowered further, more of the surfactants will be doubly protonated changing P in the direction of spherical micelles (Table 1). This fact is borne out both in theory and experiment.[8,9]

CONCLUDING REMARKS

As stated in the introductory sections, a library of sugar-based gemini surfactants with varying sugar headgroups, spacer lengths, tail lengths and chemical linkage between the headgroup and the tails, has been constructed. Work is in progress to expand this library further with the aim of fully clarifying the dependence of the aggregation behavior on the molecular structure. In particular, the negative charge of the vesicles is intriguing and it is of fundamental interest to determine the mechanism. Related to this issue, molecular dynamics (MD) simulations on bare hydrophobic surfaces in contact with water have been initiated at the University of Groningen (group of Professor A. Mark) to investigate the binding of OH^- to such surfaces. Whether or not this binding actually occurs in the gemini systems is, of course, the crucial question. However, there are many well-documented reports in the literature on this phenomenon but an explanation is still lacking.[34–38]

Some of the sugar-based gemini surfactants displayed in Fig. 1 have been shown to possess great potential as DNA carriers (transfection agents).[6,10,11] Thus a possible application is already at hand within biotechnology. Furthermore, the vesicle-to-cylindrical micelle transition within a physiologically relevant pH region may be useful for constructing acid-triggered vesicle-release systems. The scientific activities in this area are high at present and several pH-sensitive lipid vesicle formulations have been constructed aimed at a controlled release (site-specific) of vesicle-encapsulated pharmaceuticals.[44]

Acknowledgements

The authors are indebted to all co-workers on the sugar-based gemini surfactants (whose names appear in Refs 4–11). The work has been supported by the European Commission as part of its Training and Mobility of Researchers (TMR) Programme. M. J. gratefully acknowledges financial support from The Swedish Foundation for International Cooperation in Research and Higher Education (STINT).

REFERENCES

1. Menger FM, Littau CA. *J. Am. Chem. Soc.* 1991; **113**: 1451–1452.
2. Zana R. *Adv. Colloid Interface Sci.* 2002; **97**: 205–253.
3. Frindi M, Michels B, Lévy H, Zana R. *Langmuir* 1994; **10**: 1140–1145.

4. Pestman JM, Terpstra KR, Stuart MCA, van Doren HA, Brisson A, Kellogg RM, Engberts JBFN. *Langmuir* 1997; **13**: 6857–6860.
5. van Doren HA, Smits E, Pestman JM, Engberts JBFN, Kellogg RM. *Chem. Soc. Rev.* 2000; **29**: 183–199.
6. Fielden ML, Perrin C, Kremer A, Bergsma M, Stuart MCA, Camilleri P, Engberts JBFN. *Eur. J. Biochem.* 2001; **268**: 1269–1279.
7. Bergsma M, Fielden ML, Engberts JBFN. *J. Colloid Interface Sci.* 2001; **243**: 491–495.
8. Johnsson M, Wagenaar A, Engberts JBFN. *J. Am. Chem. Soc.* 2003; **125**: 757–760.
9. Johnsson M, Wagenaar A, Stuart MCA, Engberts JBFN. *Langmuir* 2003; **19**: 4609–4618.
10. Bell PC, Bergsma M, Dolbnya IP, Bras W, Stuart MCA, Rowan AE, Feiters MC, Engberts JBFN. *J. Am. Chem. Soc.* 2003; **125**: 1551–1558.
11. Kirby AJ, Camilleri P, Engberts JBFN, Feiters MC, Nolte RJM, Söderman O, Bergsma M, Bell PC, Fielden ML, García Rodríguez CL, Guédat P, Kremer A, McGregor C, Perrin C, Ronsin G, van Eijk MCP. *Angew. Chem., Int. Ed. Engl.* 2003; **42**: 1448–1457.
12. Zana R. *J. Colloid Interface Sci.* 2002; **248**: 203–220.
13. Bhattacharya S, Haldar J. *Colloids Surf., A* 2002; **205**: 119–126.
14. Menger FM, Keiper JS. *Angew. Chem., Int. Ed. Engl.* 2000; **39**: 1906–1920.
15. Hashida M, Nishikawa M, Yamashita F, Takakura Y. *Adv. Drug Delivery Rev.* 2001; **52**: 187–196.
16. Israelachvili JN, Mitchell DJ, Ninham B. *J. Chem Soc., Faraday Trans. 2* 1976; **72**: 1525–1568.
17. Gustafsson J, Orädd G, Nyden M, Hansson P, Almgren M. *Langmuir* 1998; **14**: 4987–4996.
18. Edwards K, Johnsson M, Karlsson G, Silvander M. *Biophys. J.* 1997; **73**: 258–266.
19. Israelachvili JN. *Intermolecular and Surface Forces* (2nd edn). Academic Press: San Diego, CA, 1991.
20. Almgren M, Edwards K, Karlsson G. *Colloids Surf., A* 2000; **174**: 3–21.
21. Frederik PM, Stuart MCA, Bomans PHH, Lasic DD. In *Non-medical Applications of Liposomes: Theory and Basic Sciences*, Lasic DD, Barenholz Y (eds). CRC Press: Boca Raton, FL, 1996.
22. Nagle JF, Tristram-Nagle S. *Biochim. Biophys. Acta* 2000; **1469**: 159–195.
23. Lasic DD. *Liposomes: From Physics to Applications.* Elsevier Science Publishers: Amsterdam, 1993.
24. Evans DF, Wennerström H. *The Colloidal Domain: Where Physics, Chemistry, Biology, and Technology Meet.* VCH Publishers Inc.: New York, 1994.
25. Hunter RJ. *Foundations of Colloid Science.* Oxford University Press: Oxford, 2001.
26. Frens G, Overbeek JTHG. *J. Colloid Interface Sci.* 1972; **38**: 376–387.
27. Israelachvili JN, Wennerström H. *J. Phys. Chem.* 1992; **96**: 520–531.
28. Israelachvili JN, Wennerström H. *Nature* 1996; **379**: 219–225.
29. Schneider J, Berndt P, Haverstick K, Kumar S, Chiruvolu S, Tirrell M. *Langmuir* 2002; **18**: 3923–3931.
30. Baba T, Zheng LQ, Minamikawa H, Hato M. *J. Colloid Interface Sci.* 2000; **223**: 235–243.
31. Collins KD, Washabaugh MW. *Q. Rev. Biophys.* 1985; **18**: 323–422.
32. Ninham BW, Yaminsky V. *Langmuir* 1997; **13**: 2097–2108.
33. Boström M, Williams DRM, Ninham BW. *Langmuir* 2002; **18**: 8609–8615.
34. Marinova KG, Alargova RG, Denkov ND, Velev OD, Petsev DN, Ivanov IB, Borwankar RP. *Langmuir* 1996; **12**: 2045–2051.
35. Pashley RM. *J. Phys. Chem. B* 2003; **107**: 1714–1720.
36. Bergeron V, Waltermo Å, Claesson P. *Langmuir* 1996; **12**: 1336–1342.
37. Karraker KA, Radke CJ. *Adv. Colloid Interface Sci.* 2002; **96**: 231–264.
38. Stubenrauch C, Schlarmann J, Strey R. *Phys. Chem. Chem. Phys.* 2002; **4**: 4504–4513.
39. Zheng LQ, Shui LL, Shen Q, Li GZ, Baba T, Minamikawa H, Hato M. *Colloids Surf., A* 2002; **207**: 215–221.
40. Webb MS, Tilcock CPS, Green BR. *Biochim. Biophys. Acta* 1988; **938**: 323–333.
41. Webb MS, Green BR. *Biochim. Biophys. Acta* 1990; **1030**: 231–237.
42. Gunnarsson G, Jönsson B, Wennerström H. *J. Phys. Chem.* 1980; **84**: 3114–3121.
43. Jönsson B. *PBCell.* Lund University: Lund, Sweden. (PBCell is a freeware program that can be downloaded at http://www.membfound.lth.se/chemeng1/prog.html).
44. Drummond DC, Zignani M, Leroux JC. *Prog. Lipid Res.* 2000; **39**: 409–460.

